

Effects of lattice distortion on the physical properties and surface morphology of magnetoresistive perovskite epitaxial films

N.-C. Yeh, C.-C. Fu, and J. Y. T. Wei

Department of Physics, California Institute of Technology, Pasadena, California 91125

R. P. Vasquez

Center for Space Microelectronics Technology, Jet Propulsion Laboratory, California Institute of Technology, Pasadena, California 91109

J. Huynh and S. M. Maurer

Department of Physics, California Institute of Technology, Pasadena, California 91125

G. Beach

Department of Physics, California Institute of Technology, Pasadena, California 91125 and Center for Space Microelectronics Technology, Jet Propulsion Laboratory, California Institute of Technology, Pasadena, California 91109

D. A. Beam

Department of Physics, California Institute of Technology, Pasadena, California 91125

The effects of lattice distortion on the physical properties of $\text{La}_{0.7}\text{Ca}_{0.3}\text{MnO}_3$ epitaxial films are investigated. Our results suggest that larger substrate-induced lattice distortion gives rise to larger zero-field resistivity and larger negative magnetoresistance. Similar effects are also observed in samples of different thicknesses and on the same substrate material, with larger resistivity and magnetoresistance associated with thinner samples. In addition to x-ray diffraction spectroscopy, the degrees of lattice distortion in different samples are further verified by the surface topography taken with a low-temperature scanning tunneling microscope. Quantitative analyses of the transport properties suggest that the high-temperature ($T \rightarrow T_C$) colossal magnetoresistance (CMR) in the manganites is consistent with the conduction of lattice polarons induced by the Jahn–Teller coupling, and that the low-temperature ($T \ll T_C$) magnetoresistance may be attributed to the magnetic domain wall scattering. In contrast, the absence of the Jahn–Teller coupling and the large conductivity in $\text{La}_{0.5}\text{Ca}_{0.5}\text{CoO}_3$ epitaxial films yield much smaller negative magnetoresistance, which may be attributed to disorder-spin scattering. © 1997 American Institute of Physics. [S0021-8979(97)72808-1]

Recent experimental studies of the colossal magnetoresistive manganites $\text{Ln}_{1-x}\text{A}_x\text{MnO}_{3-\delta}$ (Ln: trivalent rare earth ions; A: divalent alkaline earth ions) have led to new information which suggests the relevance of lattice effects on the conductivity and magnetism of these manganites.^{1–5} Some representative experimental observation includes a strong correlation between the thickness of epitaxial films and the corresponding magnetoresistance;¹ decreasing Curie temperatures (T_C) and increasing colossal magnetoresistance (CMR) effects with the increasing lattice distortion via the substitution of La ions by smaller ions of Pr and Y;² a significant reduction of the magnetoresistance in single crystals under a hydrostatic pressure;³ as well as a large magnetovolume effect⁴ and a giant oxygen isotope effect⁵ in $\text{La}_{1-x}\text{Ca}_x\text{MnO}_3$. On the physical origin for the CMR, the importance of lattice polaron conduction incurred by the Jahn–Teller coupling in the manganites has been proposed.⁶

In this work, we explore the correlation of the lattice distortion and Jahn–Teller coupling with the magnetoresistance of $\text{La}_{0.7}\text{Ca}_{0.3}\text{MnO}_3$ (LCMO) and $\text{La}_{0.5}\text{Ca}_{0.5}\text{CoO}_3$ (LCCO) epitaxial films. The lattice distortion is varied by either growing films of the same thickness on substrates with various lattice constants, or by varying the thickness and the growth rate of the film on the same type of substrate. The correlation between the Jahn–Teller coupling and the occurrence of CMR is investigated by comparing the physical

properties of LCMO and LCCO epitaxial films grown under the same conditions. This comparison is based on the fact that cobaltites with doping levels between 0.4 and 0.6 are known to be ferromagnetic metals, which are isostructure to the manganites and are without the Jahn–Teller coupling.^{7,8} The substrates selected include single crystalline (001) LaAlO_3 (LAO), SrTiO_3 (STO), and YAlO_3 (YAO). These substrates are chosen to provide a range of lattice constants which allows studies of the effects of tensile and compressive stress of the films.

The LCMO and LCCO epitaxial films are grown by pulsed laser deposition using stoichiometric targets. For studying the substrate-induced lattice distortion, 200 nm thick films are grown on different (001) substrates at 700 °C in 100 mTorr of oxygen, and subsequently annealed at 900 °C of 1 atm oxygen for 2 h. The Curie temperature T_C for all LCMO is 260 ± 10 K, and that for the LCCO is $T_C = 180 \pm 5$ K. The lattice constants a , b , and c ($c \perp$ sample surface) as well as the epitaxy of the films are determined using high resolution x-ray diffraction (XRD) and x-ray rocking curves, and the results have been given elsewhere.⁹ The substrate-induced lattice distortion consists of *lattice strain* and *lattice relaxation*.⁹ The former yields intrinsic effects on the phonon modes and magnetic exchange interaction, the latter yields extrinsic effects such as dislocations and domain walls. Another batch of LCMO films are grown

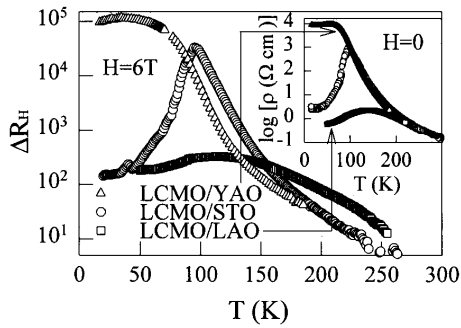


FIG. 1. The effect of lattice distortion on the magnetoresistance ΔR_H as a function of the temperature (T) is shown for $\text{La}_{0.7}\text{Ca}_{0.3}\text{MnO}_3$ epitaxial films on different substrates of LaAlO_3 , YAlO_3 , and SrTiO_3 . Here the applied field is $H=6.0$ T. The zero-field resistivity ρ vs T data for these samples are illustrated in the inset.

on LAO with a thickness of 100 nm, and under the same conditions described above except for two different growth rates controlled by the laser fluences. Among both the LCMO and LCCO films of the same thickness, we find the largest lattice distortion in LCMO/YAO and LCCO/YAO from the x-ray data.⁹ For LCMO/LAO samples with different thicknesses and under different growth rates, the thinner sample of 100 nm is found to exhibit larger lattice distortion. The chemical properties of these samples are further characterized with x-ray photoelectron spectroscopy (XPS).¹⁰ The room-temperature valence band spectroscopy shows no density of states at the Fermi level for the manganites and a high density of states at the Fermi level for the cobaltites,¹⁰ consistent with the semiconducting nature of the former and metallic nature of the latter. The effects of substrate-induced lattice strain on the optical phonon modes have been revealed by our recent infrared reflectivity studies,¹¹ and the frequency shifts of the phonon modes are consistent with the XRD results.^{9,11}

The effects of lattice distortion on the magnetoresistance ΔR_H of the LCMO films of the same thickness (200 nm) are illustrated in Fig. 1 for $H=6$ T, with the magnetoresistance in a magnetic field H defined as $\Delta R_H \equiv [\rho(c) - \rho()] / \rho(H)$. The correlation of surface topography with the magnetoresistive behavior of the sample is investigated via STM imaging. In Fig. 2 the STM surface topography of LCMO/

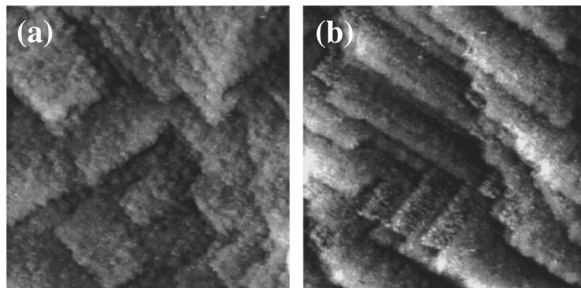


FIG. 2. STM images of 200 nm thick LCMO epitaxial films grown on (a) LAO and (b) STO substrates, showing highly oriented rectangular terraces formed by step-flow growth mode. The images are 100×100 nm in size and 1.2 nm in grey scale, indicating rms surface roughness of 0.5 nm for (a) and 0.4 nm for (b). The terrace steps are typically 0.4 nm in height, consistent with the unit cell lattice parameter.

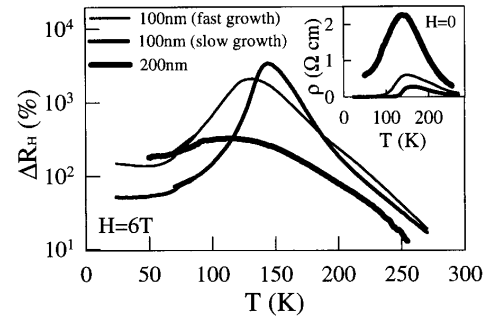


FIG. 3. Comparison of the thickness and growth rate dependence of the magnetoresistance $\Delta R_H(T)$ with $H=6.0$ T in LCMO/LAO films. The inset shows the corresponding zero-field resistivity $\rho(T)$ of the same samples.

LAO and LCMO/STO films shows images with unit-cell smooth surfaces and rectangular terraces which are oriented with respect to the substrate and the crystalline axes. According to our x-ray data and the transport measurements,⁹ the LCMO/LAO and LCMO/STO samples exhibit overall comparable lattice distortion and magnetoresistance, although the lattice distortion and the maximum magnetoresistance for LCMO/STO are slightly larger. These results are consistent with the STM surface topography in Fig. 2 which shows comparable surface roughness¹² for the two samples, with a slightly higher step density in the LCMO/STO film. Similar correlation of the surface topography with the electrical transport properties is also observed in the case of LCMO/LAO films of different thicknesses and growth rates. As illustrated in Figs. 3 and 4 the thinner (100 nm) samples show less ordered surface morphology and larger maximum magnetoresistance than the thicker sample (200 nm). It is also interesting to note that the thin sample (100 nm) under a slower growth rate (1.6 J/cm^2 laser fluence) shows both step-flow and island growth modes, whereas the faster growth rate (2 J/cm^2 laser fluence) yields a predominantly island growth mode.

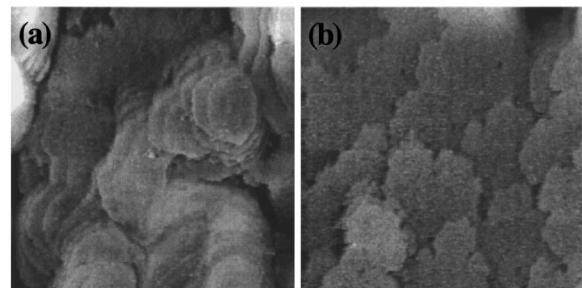


FIG. 4. STM images of 100 nm thick LCMO epitaxial films grown on LAO substrates at (a) 2 J/cm^2 and (b) 1.6 J/cm^2 laser fluence. The images are 150×150 nm in size and the grey scales are 3.5 nm for (a) and 2.5 nm for (b), with rms surface roughness of 0.7 and 0.4 nm, respectively. The higher growth-rate sample (a) shows rounded "rice-paddy" terraces indicating island growth mode. The lower growth-rate sample (b) shows ragged "fish-scale" terraces suggesting a more step-flow growth mode. The terrace steps are typically 0.4 nm in height, consistent with the unit-cell lattice parameter. The less ordered surface morphology of the 100 nm films as compared with the 200 nm films (Fig. 2) is consistent with the higher lattice distortions in the former.

Assuming polaron conduction as the dominant conduction mechanism for LCMO at high temperatures, the resistivity data for all LCMO films are analyzed according to the expression

$$\rho(T) \approx \alpha T \exp\left(\frac{E_b(T)}{k_B T}\right) \quad (1)$$

where E_b is the polaron binding energy, α a constant, and the temperature and magnetic field dependence of E_b satisfies the conditions imposed by the polaron model. That is, $E_b \rightarrow 0$ in the limit of complete magnetic order when the increasing hopping rate of the itinerant electrons exceeds the optical phonon frequency, and $E_b \rightarrow E_{b0} \sim \text{constant}$ in the absence of long-range magnetic order. For all LCMO films, the fitting to the high-temperature resistivity data yields $E_{b0} \approx 0.35$ eV.⁹ This energy compares favorably to the Jahn–Teller coupling energy,⁶ suggesting that the high-temperature conduction mechanism is dominated by the lattice polaron conduction.

On the other hand, the low-temperature transport properties appear to be strongly correlated with the degree of lattice distortion. That is, samples of larger lattice distortion exhibit larger resistivity and magnetoresistance, suggesting increasing electron scattering due to a larger number of magnetic domains and grain boundaries induced by larger lattice distortion. The incompletely aligned moments of the magnetic domains due to either inhomogeneity or pinning by local defects below T_C give rise to larger scattering of conduction electrons. Therefore, an applied magnetic field has more significant effects on aligning the magnetic domains, thereby more effectively reducing the resistivity in samples with larger lattice distortion. The substrate-induced magnetic domains and grain boundaries are uniquely associated with the epitaxial films, as evidenced by the much larger low-temperature zero-field resistivity (see the inset of Fig. 1) and the significantly enhanced low-temperature magnetoresistance (Fig. 1) relative to those of the single crystals of LCMO.¹³

To investigate the relevance of lattice polarons to the occurrence of CMR effects, the resistivity and magnetization of LCCO films on LAO and YAO substrates were studied. Despite comparable lattice relaxation and lattice strain in the manganites and in LCCO/YAO,⁹ the magnitude and temperature dependence of the resistivity in the LCMO and LCCO systems exhibit sharp contrasts, as illustrated in Figs. 1 and 5. Also shown in Fig. 5, for the LCCO/YAO sample, a faster decrease in the zero-field resistivity as well as a maximum in the magnitude of negative magnetoresistance both occur at approximately the Curie temperature ($T_C \approx 180$ K), suggesting that magnetic ordering below T_C reduces the resistivity,⁹ and that the magnetoresistance in LCCO is of the origin of spin fluctuations rather than polaron conduction.

In summary, we have studied the effects of lattice distortion on the physical properties of $\text{La}_{0.7}\text{Ca}_{0.3}\text{MnO}_3$ epitaxial films by varying the thickness of films on the same substrate, and by depositing the same thickness of films on various substrates with a range of lattice constants. Our studies reveal that larger substrate-induced lattice distortion gives rise to larger zero-field resistivity and larger negative magnetoresistance. The lattice distortion determined from the

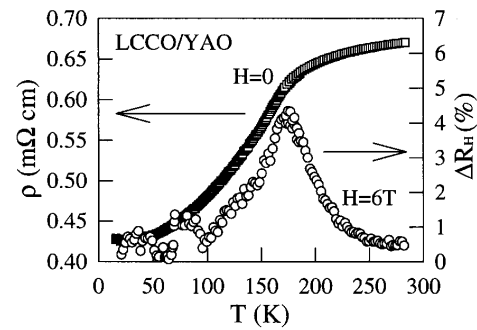


FIG. 5. The zero-field resistivity ρ and the magnetoresistance ΔR_H at $H=6$ T of a LCCO/YAO film, showing strong correlation of the magnetoresistance with spin fluctuations near T_C .

x-ray diffraction studies is further confirmed by the STM images of the surface topography. Our results suggest that the high-temperature ($T \rightarrow T_C$) CMR in the manganites is consistent with the conduction of lattice polarons induced by the Jahn–Teller coupling, and that the low-temperature ($T \ll T_C$) negative magnetoresistance can be attributed to the magnetic domain wall scattering. In contrast, the absence of the Jahn–Teller coupling and the large conductivity in $\text{La}_{0.5}\text{Ca}_{0.5}\text{CoO}_3$ epitaxial films may account for the much smaller negative magnetoresistance.

The research at Caltech is supported by the Packard Foundation and the National Aeronautics and Space Administration, Office of Space Access and Technology (NASA/OSAT). Part of the research was performed by the Center for Space Microelectronics Technology, Jet Propulsion Laboratory, Caltech, and was sponsored by NASA/OSAT. We thank Nikko Hitech International, Inc. for supplying the YAlO_3 substrates used in this work.

- ¹S. Jin, T. H. Tiefel, M. McCormack, R. A. Fastnacht, R. Ramesh, and L. H. Chen, Science **264**, 413 (1994); Appl. Phys. Lett. **66**, 382 (1995); **67**, 557 (1995).
- ²H. Y. Hwang, S.-W. Cheong, P. G. Radaelli, M. Marezio, and B. Batlogg, Phys. Rev. Lett. **75**, 914 (1995).
- ³Y. Moritomo, A. Asamitsa, and Y. Tokura, Phys. Rev. B **51**, 16 491 (1995); K. Khazeni, Y. X. Jia, L. Lu, V. H. Crespi, M. L. Cohen, and A. Zettl, Phys. Rev. Lett. **76**, 295 (1996).
- ⁴M. R. Ibarra, P. A. Algarabel, C. Marquina, J. Blasco, and J. Garcia, Phys. Rev. Lett. **75**, 3541 (1995).
- ⁵G.-M. Zhao, K. Conder, H. Keller, and K. A. Müller, Nature (London) **381**, 676 (1996).
- ⁶A. J. Millis, P. B. Littlewood, and B. I. Shraiman, Phys. Rev. Lett. **74**, 5144 (1995); A. J. Millis, B. I. Shraiman, and R. Mueller, *ibid.* **77**, 175 (1996).
- ⁷H. Ohbayashi, T. Kudo, and T. Gejo, Jpn. J. Appl. Phys. **13**, 1 (1974).
- ⁸R. Mahendiran, A. K. Raychaudhuri, A. Chainani, and D. D. Sarma, J. Phys., Condens. Matter **7**, L561 (1995); S. Yamaguchi, H. Taniguchi, H. Takagi, T. Arima, and Y. Tokura, J. Phys., Condens. Matter **64**, 1885 (1995).
- ⁹N.-C. Yeh, R. P. Vasquez, D. A. Beam, C.-C. Fu, H. Huynh, and G. Beach, (submitted to J. Phys., Condens. Matter).
- ¹⁰R. P. Vasquez, Phys. Rev. B **54**, 14 938 (1996).
- ¹¹A. V. Boris, A. V. Bazhenov, N. N. Kovaleva, A. V. Samoilov, N.-C. Yeh, and R. P. Vasquez, J. Appl. Phys. **81** (1997).
- ¹²For the definition of the surface roughness, see, for example, M. Ohring, *The Material Science of Thin Films* (Academic, San Diego, CA, 1992).
- ¹³Y. Tokura, A. Urushibara, Y. Moritomo, T. Arima, and A. Asamitsu, J. Phys. Soc. Jpn. **63**, 3931 (1994); H. Y. Hwang, S.-W. Cheong, N. P. Ong, and B. Batlogg, Phys. Rev. Lett. **77**, 2041 (1996).